Available online at www.sciencedirect.com
SCIENCE DIRECT®
Control Engineering Practice 13 (2005) 985–999
CONTROL ENGINEERING PRACTICE
www.elsevier.com/locate/conengprac

# Design of a multivariable robust controller to decrease the motion sickness incidence in fast ferries

J. Aranda[a,*], J.M. de la Cruz[b], J.M. Díaz[a]

[a] Dpt. de Informática y Automática, ETSI Informática, UNED, Juan del Rosal no 16, 28040 Madrid, Spain
[b] Dpt. de Arquitectura de Computadores y Automática, Fac. Ciencias Físicas, U. Complutense, 28040 Madrid, Spain

Received 24 November 2003; accepted 3 November 2004
Available online 15 December 2004

**Abstract**

This work serves as a pioneering contribution in the use of quantitative feedback theory methodology to the design of a controller for a high speed ship. We have improved the design of a multivariable robust controller so that it will be able to reduce incidences of motion sickness on high speed ferries. Motion sickness is caused by vertical accelerations associated with the heave and pitch motions induced by waves. Therefore we are dealing with regulation problems of a highly perturbed system. The design regulator has been validated in sea behaviour trials, using a scaled down replica $\frac{1}{25}$ the size of a high-speed ferry.


*Keywords:* Quantitative feedback theory (QFT); Robust control; Ship control

## 1. Introduction

Since the end of the Second World War, the shipping industry has focused on using light metal alloys and plastic laminates to create units that are larger and more comfortable for passengers. A striking example of these kinds of ships are the so-called Fast Ferries, used on regular lines for transporting passengers and cars. The construction and exploitation of these kinds of vehicles is a growing market, with over 200 companies using 1250 fast ferries at present. Fast ferries transported 82.6 million passengers and 12.8 million cars in Europe alone in 2000.

Sea transport's main competitor is air transport. Consequently, the keen interest of shipping companies, ship owners and builders in increasing their competitiveness with air transport is understandable.

With this in mind, the Science and Technology Ministry of Spain approved and financed a research project to investigate how modern (robust) control techniques might solve present ship control problems. One of these problems is to decrease motion sickness (Cruz et al., 2004).

One of the most unpleasant aspects of sea transport is the motion sickness suffered by both passengers and crew. This is a result of the vertical accelerations associated with the induced heave and pitch motions. Our goal is to decrease motion sickness as much as possible.

A ferry subjected to waves behaves like a highly perturbed system. Therefore a robust multivariable regulator must be designed that can control the motion of the right mechanical actuators (flaps, T-foil, etc.), and is able to attenuate the ferry's vertical dynamic motions (heave and pitch) as far as possible. Reducing these associated vertical accelerations thereby minimizes motion sickness incidence (MSI), the measurement used for quantifying motion sickness suffered by passengers.

*Corresponding author. Tel: +34 91 398 71 48; fax: +34 91 398 66 97.
*E-mail address:* jaranda@dia.uned.es (J. Aranda).

0967-0661/$ - see front matter © 2004 Elsevier Ltd. All rights reserved.
doi:10.1016/j.conengprac.2004.11.003

Quantitative feedback theory (QFT) was created and developed by Horowitz (1963). It is a frequency domain design technique, which allows robust controllers to fulfil some minimum features, formulated quantitatively, taking into consideration the existence of plant model uncertainties and perturbations. QFT methodology has been successfully applied to solve different control problems in various fields of engineering (Horowitz, 1992, 2001; Houpis, Sating, Rasmussen, & Sheldon, 1994; Houpis & Rasmussen, 1999; Yaniv, 1999).

This work presents for the first time, the design of a multivariable robust regulator with QFT methodology used for the reduction of motion sickness incidence on a high-speed ferry. The designed regulators are tested in sea behaviour trials, using a scaled down replica $\frac{1}{25}$ the size of a high-speed ferry.

The structure of this work is the following: Process models are considered in Section 2. Motion sickness incidence (MSI) is defined in Section 3. The design of a multivariable robust regulator using QFT methodology, and how it is used for the reduction of motion sickness incidence on a high speed ferry is described in Section 4. The experiments that were conducted to test this design are described in Section 5. Finally, the conclusions are collected in Section 6.

## 2. Process model

Continuous models of the vertical dynamics (heave and pitch) of a high-speed ferry referring to the bow at different navigation speeds ($U = 20$, 30 and 40 knots) are used. These models were obtained by means of identification techniques in the frequency domain (Aranda, Cruz, & Díaz, 2004). Vertical dynamics models refer to the bow because wave perturbation generates unstable models if they are measured from the centre of gravity.

These models can be considered as acceptable since they adjust well to the amplitude and phase of the experimental data. Their time simulations both with regular and irregular waves, present only a small average quadratic error when compared with the experimental time series.

Two kinds of mechanical actuators were designed (see Fig. 1), a pair of fins on bow (T-foil) and two flaps on stern (flaps). Both linear and nonlinear models were obtained for these actuators (Esteban et al., 2000).

The process model is taken to be the linear model of the vertical dynamics of a high-speed ferry together with the non-linear model of the actuators. This is a multivariable model with two manipulated variables: the set-point of the

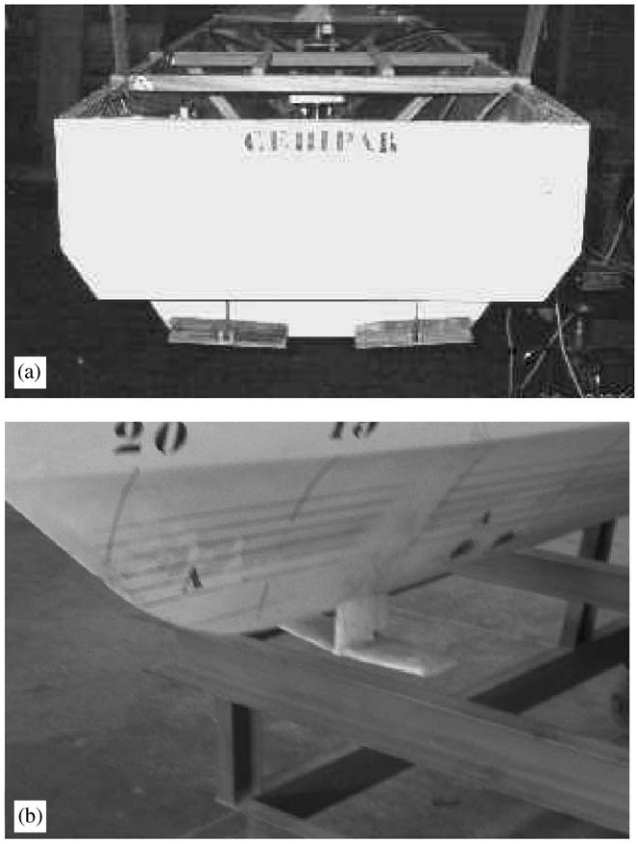


Fig. 1. Mechanical actuators of the scaled down replica $\frac{1}{25}$ the size of a fast ferry: (a)Two flaps on stern. (b) T-foil on bow.

flaps position $u_F$ and the set-point of the T-foil position $u_T$. The process has two controlled variables: the heave motion $h$ and the pitch motion $p$. There is also one disturbance: wave height $w$.

If the saturation of the actuators is not very high, a linear model of the actuators for position control can be considered (Esteban et al., 2000). In this case it is possible to represent the process using the following equation:

$$\mathbf{y} = \mathbf{P} \cdot \mathbf{u} + \mathbf{d} \tag{1}$$

where $\mathbf{y}$ is the output vector, $\mathbf{u}$ is the control vector, $\mathbf{d}$ is the disturbance vector and $\mathbf{P}$ is the plant. This process is a multiple input-multiple output (MIMO) $2 \times 2$ process, so Eq. (1) can be written in the form

$$\begin{bmatrix} h(s) \\ p(s) \end{bmatrix} = \begin{bmatrix} P_{FH}(s) & P_{TH}(s) \\ P_{FP}(s) & P_{TP}(s) \end{bmatrix} \begin{bmatrix} u_F(s) \\ u_T(s) \end{bmatrix} + \begin{bmatrix} d_{WH}(s) \\ d_{WP}(s) \end{bmatrix}. \tag{2}$$

Or equivalently in the form

$$\begin{bmatrix} h(s) \\ p(s) \end{bmatrix} = \begin{bmatrix} P_{FH}(s) & P_{TH}(s) \\ P_{FP}(s) & P_{TP}(s) \end{bmatrix} \begin{bmatrix} u_F(s) \\ u_T(s) \end{bmatrix} + \begin{bmatrix} P_{WH}(s) \\ P_{WP}(s) \end{bmatrix} w(s), \tag{3}$$

where $P_{ij}(s)$ are transfer functions from outputs $j = \{h, p\}$ to inputs $i = \{u_F, u_T, w\}$.

A family of plants $\mathscr{P}$ defined as transfer function with parametric uncertainties in its coefficients was obtained in Díaz (2002) from the linear model of the process at different ship speeds (20, 30 and 40 knots). Its expression is

$$\mathscr{P} = \begin{pmatrix} K_{FH} \dfrac{(s^2 + a_1 s + b_1)}{(s + 103.9)(s + 1.8)(s^2 + c_1 s + d_1)} & K_{TH} \dfrac{(s^2 + a_1 s + b_1)}{(s + 103.9)(s + 1.8)(s^2 + c_1 s + d_1)} \\ K_{FP} \dfrac{(s + a_2)(s + b_2)}{(s + 103.9)(s + 1.8)(s + c_2)(s^2 + d_2 s + e_2)} & K_{TP} \dfrac{(s + a_2)(s + b_2)}{(s + 103.9)(s + 1.8)(s + c_2)(s^2 + d_2 s + e_2)} \end{pmatrix}, \tag{4}$$

where

$$\begin{gathered} K_{FH} \in [0.16, 0.23], \quad K_{TH} \in [-0.21, -0.15], \quad K_{FP} \in [-0.63, -0.45], \quad K_{TP} \in [-0.87, -0.65], \\ a_1 \in [-1.91, -1.45], \quad b_1 \in [8.31, 11.45], \quad c_1 \in [0.47, 0.49], \quad d_1 \in [2.86, 3.07], \\ a_2 \in [-7.85, -6.68], \quad b_2 \in [0.026, 0.042], \quad c_2 \in [0.44, 0.49], \quad d_2 \in [0.86, 0.98], \quad e_2 \in [2.59, 2.81]. \end{gathered} \tag{5}$$

The nominal plant $\mathbf{P}_0 \in \mathscr{P}$ is chosen at a ship speed of 40 knots, a case of special interest for navigation. Its expression is

$$\mathbf{P_0} = \begin{bmatrix} P^0_{FH}(s) & P^0_{TH}(s) \\ P^0_{FP}(s) & P^0_{TP}(s) \end{bmatrix}, \tag{6}$$

where

$$P^0_{FH}(s) = \frac{0.23\left(s^2 - 1.911s + 11.45\right)}{(s + 103.9)(s + 1.8)(s^2 + 0.4922s + 3.074)}, \tag{7}$$

$$P^0_{TH}(s) = \frac{-0.208\left(s^2 - 1.911s + 11.45\right)}{(s + 103.9)(s + 1.8)(s^2 + 0.4922s + 3.074)}, \tag{8}$$

$$P^0_{FP}(s) = \frac{-0.6305(s - 7.855)(s + 0.0417)}{(s + 103.9)(s + 1.8)(s + 0.4915)(s^2 + 0.8614s + 2.807)}, \tag{9}$$

$$P^0_{TP}(s) = \frac{-0.87(s - 7.855)(s + 0.0417)}{(s + 103.9)(s + 1.8)(s + 0.4915)(s^2 + 0.8614s + 2.807)}. \tag{10}$$

The family of plants $\mathscr{P}$ has 13 independent parameters. Moreover, a family $\mathscr{D}$ of transfer functions $P_{WH}$ and $P_{WP}$ associated to the perturbation $w$ with 28 independent parameters can also be obtained (Díaz, 2002). Therefore, the system will have a total of 41 parameters. Working with such a high number of parameters makes it extremely complicated to obtain templates, which are going to be used in the QFT design to generate the different bounds associated with the specifications. A good approximation (Díaz, 2002) is to consider that the transfer functions $P_{WH}$ and $P_{WP}$ associated with the perturbations are fixed, i.e., the family of perturbations $\mathscr{D}$ only consists of one member,

choosing for the design the expressions in the nominal conditions given by the equations

$$P_{WH}(s) = \frac{1.8(s-0.2036)(s^2+1.039s+2.504)C_1(s)C_2(s)}{(s+103.9)(s^2+0.4367s+0.1071)C_3(s)C_4(s)},$$
$$C_1(s) = (s^2-1.911s+11.45)(s^2+1.646s+14.62)$$
$$C_2(s) = (s^2+0.7292s+3.495)$$
$$C_3(s) = (s^2+0.9037s+1.764)(s^2+0.8614s+2.807)$$
$$C_4(s) = (s^2+1.177s+3.157)(s^2+0.4922s+3.074) \quad (11)$$

$$P_{WP}(s) = \frac{16.0545s(s-7.855)(s+0.0417)D_1(s)}{(s+100)(s+0.9272)(s+0.9244)(s+4915)D_2(s)}.$$
$$D_1(s) = (s^2-0.3942s+12.14)$$
$$D_2(s) = (s^2+0.8614s+2.807)(s^2+1.177s+3.157) \quad (12)$$

## 3. Motion sickness incidence

The motion sickness that people suffer when they travel by ship is due to the vertical acceleration associated with the heave and pitch motions induced by the waves. The organs of balance located in the inner ear can detect changes in the magnitude and direction of gravitational and angular accelerations.

The quantification of motion sickness is a complicated problem, since the vertical accelerations that cause it affect every individual differently. It is necessary to use statistical methods, and consider a large number of analysed subjects. A classic experiment on sea motion sickness is presented in O'Hanlon and McCauley (1974), who defined MSI as the percentage of subjects that had become sick during 2 h of navigation. They expressed it mathematically as

$$\mathrm{MSI} = 100\left[0.5 + erf\left(\frac{\log_{10}\left(\frac{WVA}{g}\right) - \mu_{\mathrm{MSI}}}{0.4}\right)\right], \quad (13)$$

where $WVA$ is the average value of the total vertical acceleration $a_V$ at 40 m ahead of the mass centre for a total of $N$ points.

$$WVA = \frac{1}{N}\sum_{i=1}^{N}\left|a_V(t_i)\right|. \quad (14)$$

Moreover $\mu_{\mathrm{MSI}}$ in Eq. (13) is defined by the equation

$$\mu_{\mathrm{MSI}} = -0.819 + 2.32\,(\log_{10}\omega_e)^2 \quad (15)$$

where $\omega_e$ is the wave encounter frequency, which is the relative frequency with which the waves fall against a ship.

Fig. 2 shows the MSI value for different $WVA$ amplitudes according to the wave encounter frequency. It should be highlighted that the maximums of MSI occur around a frequency $\omega_e = 1.07$ rad/s, and as the acceleration increases, the number of people who suffer motion sickness increases. Minimizing MSI implies reducing $WVA$. Therefore, the heave and pitch motions induced by the waves will be reduced as well.

From the study of the dominant wave encounter frequency component in each sea state, and from the study of the wave spectrum, it can be deduced that the right range of frequencies to minimize MSI as far as possible is $\Omega = [1, 2.5]$ rad/s.

## 4. Controller design

This section describes the QFT design of a multivariable robust control scheme acting on T-foil and flaps to reduce MSI on a high-speed ferry. The validation of the proposed design is also included.

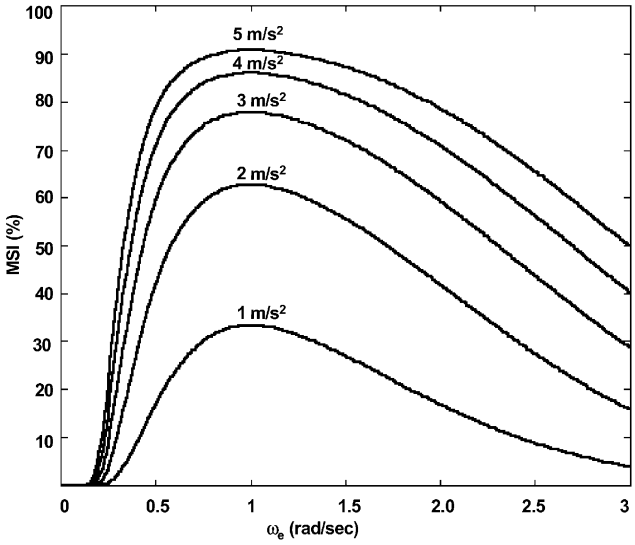


Fig. 2. Motion sickness incidence MSI for different *WVA*.

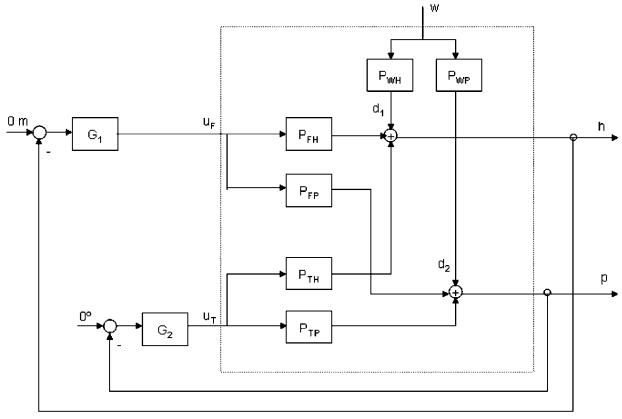


Fig. 3. Scheme of robust regulation used for the linearised process.

### 4.1. Statement of the control problem

QFT methodology allows robust controllers to be designed for MIMO systems (Horowitz, 1992; Houpis & Rasmussen, 1999; Yaniv, 1999), both for tracking and regulation problems. Basically, the usual form of solving a control problem for a $m \times m$ MIMO system with QFT is to transform it into $m^2$ problems for $m \times 1$ MISO systems. In the case of a regulation problem for a $2 \times 2$ MIMO system, just transforming it into two single input-single output (SISO) problems is sufficient.

The feedback system under consideration is schematically described in Fig. 3. The outputs $h(s)$ and $p(s)$ are defined by the following expression:

$$\begin{bmatrix} h(s) \\ p(s) \end{bmatrix} = \left( \begin{bmatrix} 1 & 0 \\ 0 & 1 \end{bmatrix} + \begin{bmatrix} P_{FH}(s) & P_{TH}(s) \\ P_{FP}(s) & P_{TP}(s) \end{bmatrix} \begin{bmatrix} G_1(s) & 0 \\ 0 & G_2(s) \end{bmatrix} \right)^{-1} \begin{bmatrix} P_{WH}(s) \\ P_{WP}(s) \end{bmatrix} w(s). \tag{16}$$

Making some computations (Yaniv, 1999) the outputs can be expressed in the form

$$h = \frac{Q_{11} \cdot P_{WH} \cdot w + Q_{12} \cdot P_{WP} \cdot w - Q_{12} \cdot p}{Q_{11} + G_1}, \tag{17}$$

$$p = \frac{Q'_{21} \cdot P_{WH} \cdot w + Q'_{22} \cdot P_{WP} \cdot w}{Q'_{22} + G_2}, \tag{18}$$

where

$$\left[Q_{ij}\right] = \begin{bmatrix} Q_{11} & Q_{12} \\ Q_{21} & Q_{22} \end{bmatrix} = \mathbf{P}^{-1}, \tag{19}$$

$$Q'_{21} = Q_{21} - \frac{Q_{21} \cdot Q_{11}}{Q_{11} + G_1} = \frac{Q_{21} G_1}{Q_{11} + G_1}, \tag{20}$$

$$Q'_{22} = Q_{22} - \frac{Q_{21} \cdot Q_{12}}{Q_{11} + G_1}. \tag{21}$$

The sensitivity $S_{PW}$ of the output $p$ to the perturbation $w$ is

$$S_{WP}(s) = \frac{p(s)}{w(s)} = \frac{Q'_{21}(s) P_{WH}(s) + Q'_{22}(s) P_{WP}(s)}{Q'_{22}(s) + G_2(s)}. \tag{22}$$

While the sensitivity $S_{HW}$ of the output $h$ to the perturbation $w$ is

$$S_{WH}(s) = \frac{h(s)}{w(s)} = \frac{Q_{11}(s) P_{WH}(s) + Q_{12}(s) P_{WP}(s) - Q_{12}(s) S_{WP}(s)}{Q_{11}(s) + G_1(s)}. \tag{23}$$

The problem to solve may be formally stated as follows:

Problem MIMO. Consider the system shown in Fig. 3. Design the controller $\mathbf{G} = \mathrm{diag}(G_1, G_2)$ such that for all $\mathbf{P} \in \mathscr{P}$ the system is stable, and for all disturbance $\mathbf{d} \in \mathscr{D}$ and frequency $\omega \in \Omega$ the magnitude of the sensitivity functions $S_{WH}$ and $S_{WP}$ are bounded by the specifications $W_{WH}$ and $W_{WP}$ ,respectively:

$$\left|S_{WH}(j\omega)\right| \leqslant W_{WH}(\omega) \tag{24}$$

$$\left|S_{WP}(j\omega)\right| \leqslant W_{WP}(\omega) \tag{25}$$

In Yaniv (1999) it is shown that the QFT design of the controllers $G_1$ and $G_2$ are such that a MIMO $2 \times 2$ system presents robust stability and robust behaviour for every plant $\mathbf{P} \in \mathscr{P}$ and for every perturbation $\mathbf{d} \in \mathscr{D}$. This can also be done by solving sequentially the following two SISO regulation problems:

Problem SISO 1. Consider the SISO 1 system shown in Fig. 4. The plant $P_{e1}$ is defined by the following equation:

$$P_{e1} = \frac{1}{Q_{11}}. \tag{26}$$

The problem outlined is to design $G_1$ such that for all $\mathbf{P} \in \mathscr{P}$ the system is stable and for all disturbance $\mathbf{d} \in \mathscr{D}$ and frequency $\omega \in \Omega$ the sensitivity function $S_{WH}$ are bounded by (24).

The expression (23) of $S_{WH}$ is a function of $S_{WP}$, which cannot be determined until $G_2$ is designed. Nevertheless, according to (22) $S_{WP}$ is also bounded by $W_{WP}$ which must also be specified a priori. Therefore Eq. (23) can be expressed by

$$\left|S_{WH}(j\omega)\right| \leqslant \frac{\left|Q_{11}(j\omega) P_{WH}(j\omega) + Q_{12}(j\omega) P_{WP}(j\omega)\right| + \left|Q_{12}(j\omega) W_{WP}(\omega)\right|}{\left|Q_{11}(j\omega) + G_1(j\omega)\right|} \leqslant \left|W_{WH}(\omega)\right|. \tag{27}$$

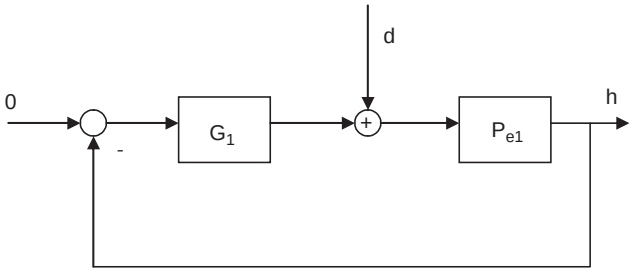


Fig. 4. SISO 1 feedback system.

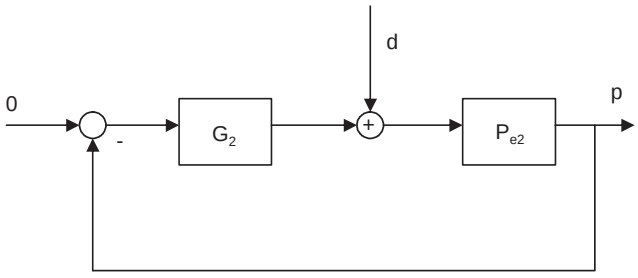


Fig. 5. SISO 2 feedback system.

Problem SISO 2. Consider the SISO system shown in Fig. 5. The plant $P_{e2}$ is defined by the following equation:

$$P_{e2} = \frac{1}{Q'_{22}}. \tag{28}$$

The problem outlined is to design $G_2$ such that for all $\mathbf{P} \in \mathscr{P}$ the system is stable and for all disturbance $\mathbf{d} \in \mathscr{D}$ and frequency $\omega \in \Omega$ the sensitivity function $S_{WP}$ are bounded by (25).

### 4.2. Specifications

In accordance with Eq. (13), a decrease in $WVA$ produces some decrease in MSI. Therefore the heave and pitch motions induced on the ship by the waves must be reduced as far as possible, since they are primarily responsible for the vertical acceleration.

The decrease in heave and pitch motions is equivalent to reducing the system's sensitivity to the waves. From the point of view of frequency domain this means working with the sensitivity functions $S_{WH}$ and $S_{WP}$, defined in the Eqs. (27) and (22), respectively. The more negative the magnitude in decibels of both functions in the range of frequencies $\Omega$ considered, the greater the perturbation rejection that is going to be obtained, and therefore the greater the reduction in MSI.

The key for establishing this perturbation rejection specification is to appropriately fix analytically or numerically $W_{WH}(\omega)$ and $W_{WP}(\omega)$, i.e., impose some higher bounds for $|S_{WH}|$ and $|S_{WP}|$ that guarantee the following conditions for every plant $\mathbf{P} \in \mathscr{P}$ and for every perturbation $\mathbf{d} \in \mathscr{D}$:

(1) Maximum reduction possible in MSI within a set range of frequencies $\Omega$.
(2) Robust stability of the system.

There is no analytical expression that relates MSI with $|S_{WH}|$ and $|S_{WP}|$. Therefore it is neither direct nor trivial to ascertain what MSI reduction percentage will be achieved for some set functions $S_{WH}$ and $S_{WP}$. Therefore the method has to be indirect using approximation. It is obvious that given a controller $\mathbf{G}$, with each one of the plants $\mathbf{P} \in \mathscr{P}$, a reduction percentage in MSI will be obtained. If the controller is robust it must ensure a minimum percentage irrespective of the $\mathbf{P} \in \mathscr{P}$ considered.

Nevertheless, $W_{WH}(\omega)$ and $W_{WP}(\omega)$ cannot be chosen so that $|S_{WH}|$ and $|S_{WP}|$ are arbitrarily small, because the system presents two important limitations: the family of plants $\mathscr{P}$ is non-minimum phase (NMP), and the saturation of the actuators.

The family of plants $\mathscr{P}$ (see Eq. (4)) has zeros in the right half of the complex plane. The benefits of feedback for NMP plants are limited, in the sense that not any closed loop specifications can be achieved using a linear time invariant controller. The open loop crossover frequency of an NMP system has an upper bound (Horowitz, 1992; Yaniv, 1999), hence the amplitude of the open loop frequencies below the cross-over frequency is also bounded. This limitation is clearly shown in the loop shaping stage of the QFT methodology in the resolution of the problem SISO 1 and SISO 2. If $W_{WH}(\omega)$ and $W_{WP}(\omega)$ are chosen so that $|S_{WH}|$ and $|S_{WP}|$ are too small, the disturbance rejection bounds in the Nichols chart will be far away from the 0 dB axis and it will not be possible to find a controller that can fulfil this specification without making the system unstable.

The saturation of the actuators is a factor that must be taken into account when $W_{WH}(\omega)$ and $W_{WP}(\omega)$ are chosen. This is because the larger the perturbation rejection, the greater the saturation that will be obtained—negating the benefits of the feedback.

Table 1
Specifications $W_{WH}(\omega)$ and $W_{WP}(\omega)$

| $\omega$ (rad/s) | $W_{WH}$ (dB) | $W_{WP}$ (dB) |
|---|---|---|
| 1.00 | −0.20 | 2.00 |
| 1.25 | 0.60 | 3.00 |
| 1.50 | 1.00 | 3.10 |
| 2.00 | −2.30 | −4.75 |
| 2.50 | −18.0 | −18.5 |

A good starting point for the selection of $W_{WH}$ and $W_{WP}$ is to consider the sensitivity functions $S_{WH}$ and $S_{WP}$ (Eqs. (27) and (22)) that are obtained when the process is controlled with a gain-scheduling scheme using PD controllers (Aranda, Díaz, Ruipérez, Rueda, & López, 2001), and ship speeds of $U = 20, 30, 40$ knots. With these PD controllers, some acceptable reductions in MSI were obtained. For example, at nominal conditions the PD controllers are

$$G_1 = \frac{0.50s + 1.13}{0.04s + 1}, \quad G_2 = \frac{10.84s + 7.79}{0.12s + 1}. \tag{29}$$

And a MSI reduction percentage of about 81% is obtained.

Thus, bearing in mind the conditions to fulfil and the limitations to consider, an iterative trial and error method was used to select $W_{WH}$ and $W_{WP}$. The selected $W_{WH}$ and $W_{WP}$ are shown in Table 1.

According to Yaniv (1999) a possible form to assure the robust stability of the system is to fulfil the following specification in the resolution of the Problem SISO 1:

$$\left|\frac{1}{1 + G_1 \cdot P_{e1}}\right| \leqslant W_{e1}, \quad \forall \mathbf{P} \in \mathscr{P}, \quad \forall \omega \geqslant \omega_h. \tag{30}$$

And the following specifications in the resolution of the Problem SISO 2:

$$\left|\frac{1}{1 + G_2 \cdot P_{e2}}\right| \leqslant W_{e2}, \quad \forall \mathbf{P} \in \mathscr{P}, \quad \forall \omega \geqslant \omega_h. \tag{31}$$

$W_{e1}$ and $W_{e2}$ are constant values that must be larger than 1.

Specifications (30) and (31) draw closed bounds $B(\omega_i)\omega_i \geqslant \omega_h$ in the Nichols Chart around the critical point (−180°, 0 dB). These bounds are very useful in the loop-shaping stage as a visual reference so that the open loop does not enter into the forbidden zone of the Nichols (phases less than −180° and magnitude larger than 0 dB) and secure some stability margin. For this system, according to the range of frequencies $\Omega$ defined in Section 3, $\omega_h$ is chosen to be 2.5 rad/s. Several previous trial and error iterations showed that a good selection is $W_{e1} = W_{e2} = 1.8$.

### 4.3. Synthesis of the controller

In accordance with Section 4.1, the controller $G_1$ is obtained from the solution of the regulation problem SISO 1. The nominal plant $P^0_{e1}$ is given by the following transfer function:

$$P^0_{e1}(s) = \frac{0.38s^2 - 0.73s + 4.37}{s^4 + 106.9s^3 + 241.88s + 416.14s + 574.15}. \tag{32}$$

From the adjustment of the open-loop function $L_1(j\omega) = G_1(j\omega) \cdot P^0_{e1}(j\omega)$ over the final bounds $B_1(\omega)$ defined for the specifications (27) and (30) in the Nichols chart, the controller $G_1$ is obtained (see Fig. 6).

$$G_1(s) = 88.58 \cdot \frac{\left(\frac{s^2}{1.74^2} + \frac{2 \cdot 0.65}{1.74}s + 1\right)\left(\frac{s^2}{4.27^2} + \frac{2 \cdot 0.37}{4.27}s + 1\right)}{\left(\frac{s^2}{4.30^2} + \frac{2 \cdot 0.25}{4.30}s + 1\right)\left(\frac{s}{8} + 1\right)\left(\frac{s^2}{100^2} + \frac{2 \cdot 0.5}{100}s + 1\right)}. \tag{33}$$

Moreover, the controller $G_2$ is obtained from the solution of the regulation problem SISO 2. The nominal plant $P^0_{e2}$ is given by the following transfer function:

$$P^0_{e2}(s) = -0.87\frac{(s - 7.855)(s + 0.041)}{(s + 103.9)(s + 1.8)(s + 0.491)(s^2 + 0.861s + 2.807)}. \tag{34}$$

From the adjustment of the open-loop function $L_2(j\omega) = G_2(j\omega) \cdot P_{e2}^0(j\omega)$ over the final bounds $B_2(\omega)$ defined for the specifications (23) and (31) in the Nichols chart, the controller $G_2$ is obtained (see Fig. 7).

$$G_2(s) = 35.03 \cdot \frac{\left(\frac{s^2}{1.74^2} + \frac{2 \cdot 0.65}{1.74}s + 1\right)\left(\frac{s}{2.14} + 1\right)\left(\frac{s^2}{4.34^2} + \frac{2 \cdot 0.27}{4.34}s + 1\right)}{\left(\frac{s^2}{4.30^2} + \frac{2 \cdot 0.25}{4.30}s + 1\right)\left(\frac{s}{10.2} + 1\right)\left(\frac{s}{38.6} + 1\right)\left(\frac{s^2}{100^2} + \frac{2 \cdot 0.5}{100}s + 1\right)}. \tag{35}$$

The calculation of the templates and the bounds were done with the Matlab QFT toolbox (Borghesani, Chait, & Yaniv, 1995). Calculating of the approximations of the templates was done using a parameter space sweep method, where a total of 1301 plants were used. In the loop shaping stage, to compute $G_1$ and $G_2$ the software tool IDESQLS (interactive design environment in SysQuake for loop-shaping) (Dormido, Aranda, Díaz, & Dormido Canto, 2001) was used, which is an interactive design environment for adjustment of the loop function constructed in Sysquake (Piguet, 1999).

### 4.4. Validation of the designed controller

Once both of the elements $G_1$ and $G_2$ of the controller G have been obtained, the design has to be validated. The validation of the specifications (24) and (25) was done using 2602 plants $\mathbf{P} \in \mathscr{P}$. These plants are the sum of the 1301 plants $\mathbf{P} \in \mathscr{P}$ used to calculate the templates and 1301 plants $\mathbf{P} \in \mathscr{P}$ randomly chosen (Vidyasagar, 2001).

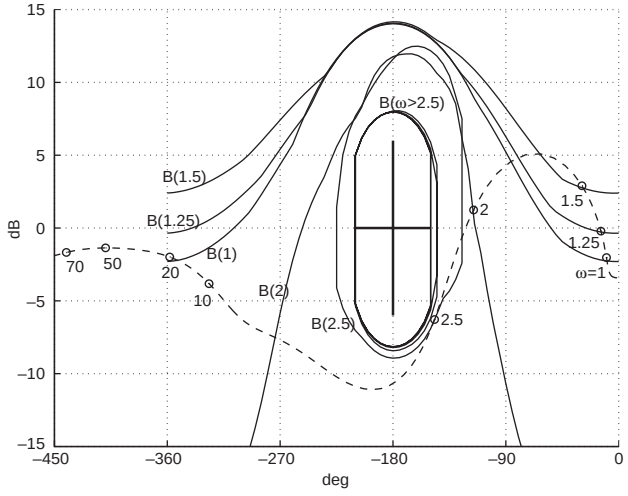


Fig. 6. $L_1(j\omega)$ (broken line) and its bounds $B_1(\omega)$ for the nominal case.

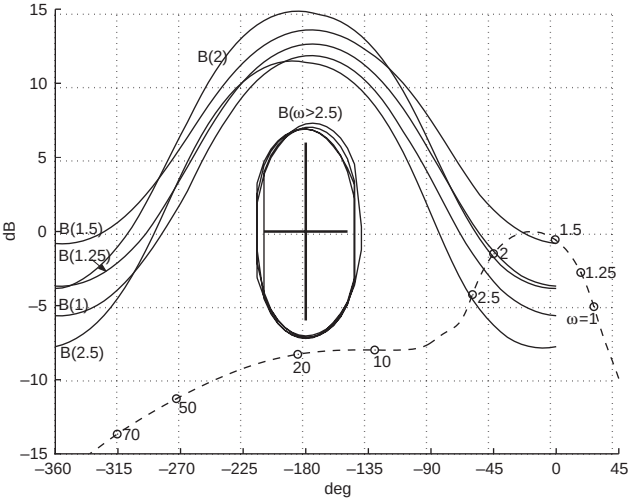


Fig. 7. $L_2(j\omega)$ (broken line) and its bounds $B_2(\omega)$ for the nominal case.

Fig. 8 represents $max\{|S_{WH}(j\omega)|\}$, the maximum magnitude of the sensitivity function $S_{WH}(j\omega)$, for 2602 plants $\mathbf{P} \in \mathscr{P}$ and the specification $W_{WH}(\omega)$. The specification is fulfilled, since $max\{|S_{WH}(j\omega)|\}$ is always below of $W_{WH}$ in the range of frequencies $\Omega$.

Furthermore, Fig. 9 represents $max(|S_{WP}(j\omega)|)$ the maximum magnitude of the sensitivity function for 2602 plants $\mathbf{P} \in \mathscr{P}$ and the specification $|W_{WP}(j\omega)|$. The fulfilment of the specification is observed, since $max\{|S_{WP}(j\omega)|\}$ is always below $|W_{WP}|$ in the range of frequencies $\Omega$.

The time simulation of the nonlinear controlled process is done with the designed regulator $\mathbf{G}$. Four working points are considered (ship speed $U = 30$, 40 knots and sea state number SSN = 4, 5). Table 2 shows the $WVA$ and MSI reduction percentages obtained. In Fig. 10, the vertical acceleration obtained in simulation at the nominal conditions ($U = 40$ knots, SSN = 4) of the process, with and without control from the regulator $\mathbf{G}$ is shown. A 29.2% reduction in $WVA$ is achieved using this regulator.

It is also interesting to compare the $WVA$ and MSI reduction percentages obtained in the simulation of the nonlinear process using the gain scheduling scheme with PD obtained in Aranda et al. (2001), with the controller $\mathbf{G}$ obtained using QFT. Table 3 shows how the reductions in MSI that are achieved with the gain scheduling scheme with PD are higher than those obtained with the controller $\mathbf{G}$ obtained using QFT. This behaviour is basically to be expected since the controller $\mathbf{G}$ is designed to be robust, ensuring a minimum in the MSI reduction percentage for a set of plants $\mathbf{P} \in \mathscr{P}$. In other words, the QFT design implies working with the worst case scenario. While the gain scheduling scheme is tuned optimally on just four working points.

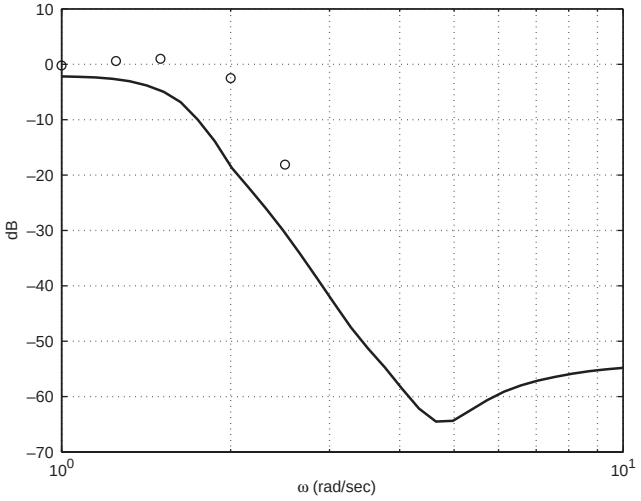


Fig. 8. Maximum magnitude of the sensitivity $S_{WH}(j\omega)$ for 2602 plants $\mathbf{P} \in \mathscr{P}$ and the specification $W_{WH}(\omega)$ (circular points).

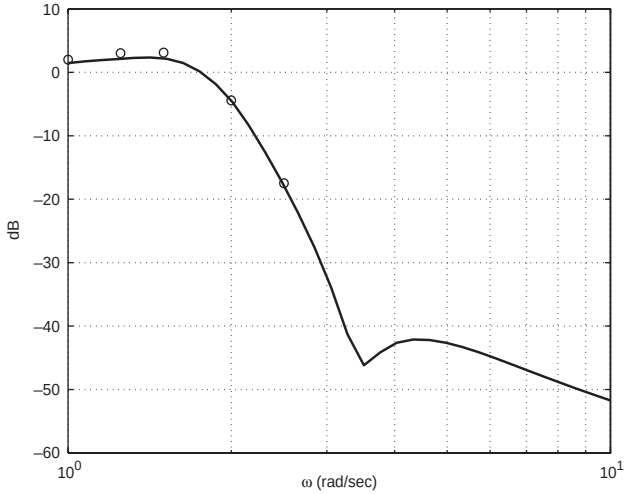


Fig. 9. Maximum magnitude of the sensitivity $S_{WP}(j\omega)$ for 2602 plants $\mathbf{P} \in \mathscr{P}$ and the specification $W_{WH}(\omega)$ (circular points).

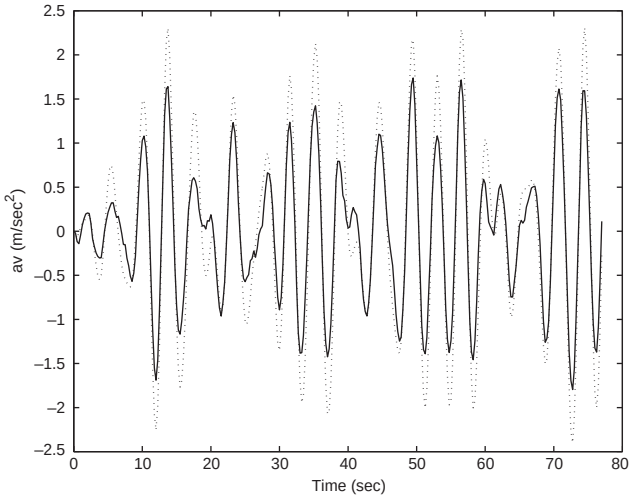


Fig. 10. Vertical acceleration obtained in time simulation at $U = 40$ knots and SSN = 4 of the process without control (broken line) and controlled (solid line) with the controller **G**.

Table 2
*WVA* and MSI reduction percentages obtained in simulation

| (*U*,SSN) | *WVA* (%) | MSI (%) |
|---|---|---|
| (30,4) | 23.3 | 45.0 |
| (30,5) | 11.6 | 12.1 |
| (40,4) | 29.2 | 51.9 |
| (40,5) | 16.0 | 14.7 |

Table 3
Reduction percentages of the MSI obtained in the simulation of the nonlinear process using a gain scheduling scheme with PD and the designed controller **G**

| (*U*,SSN) | MSI(PD) (%) | MSI(**G**) (%) |
|---|---|---|
| (30,4) | 79.9 | 45.0 |
| (30,5) | 45.8 | 12.1 |
| (40,4) | 81.0 | 51.9 |
| (40,5) | 47.4 | 14.7 |

In order to complete the comparison, μ-analysis was used to validate the robust stability and performance of the process controlled with the regulator **G**, and with a gain scheduling scheme with PD.

In Fig. 11, the upper bound of the structured singular value μ obtained in the study of the robust stability of the process controlled using the gain scheduling scheme with PD, and controlled by the regulator **G** is shown. It can be observed that the system controlled with both of these controllers has maintained robust stability in the face of all variations to the parameters of the process because $\mu < 1$ for all the frequencies.

Moreover, in Fig. 12 it is shown the lower bound of the structured singular value μ obtained in the study of the robust performance of the process controlled with the gain scheduling scheme with PD and controlled with the regulator **G**. It can be observed that the system controlled by the gain scheduling scheme using PD has not got robust performance in the face of variations to the parameters of the process because $\mu > 1$ for all the frequencies. Nevertheless, the system controlled with the regulator **G** has got robust performance in the face of variations to the parameters of the process because $\mu < 1$ in the range of design $\Omega$.

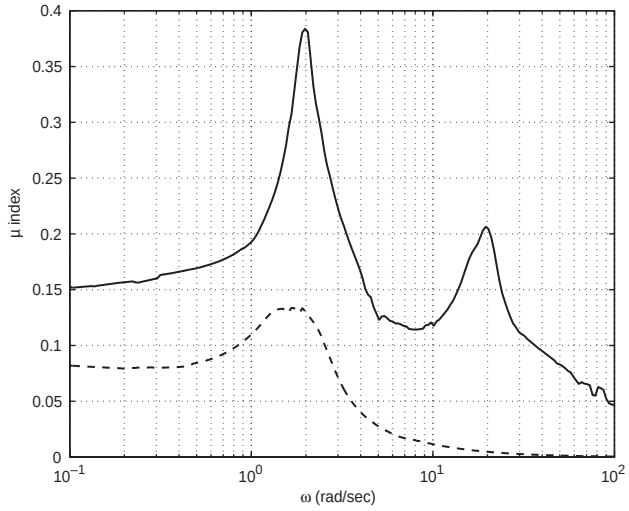


Fig. 11. Upper bound of the structured singular value $\mu$ obtained in the study of the robust stability of the process controlled with a gain scheduling scheme with PD (broken line) and controlled (solid line) with the regulator **G**.

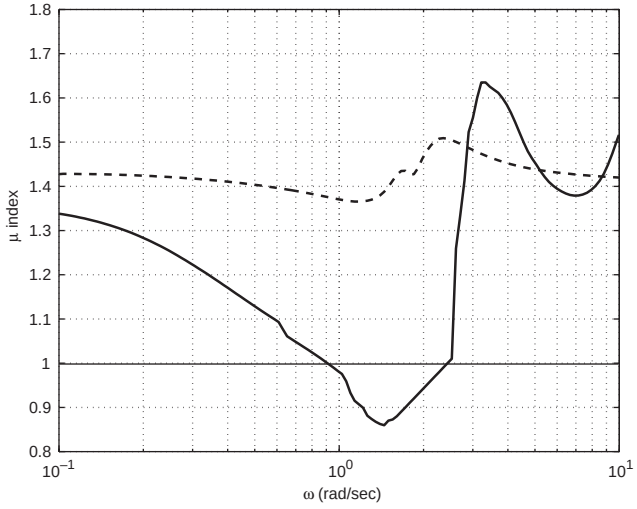


Fig. 12. Lower bound of the structured singular value $\mu$ obtained in the study of the robust performance of the process controlled with a gain scheduling scheme with PD (broken line) and controlled (solid line) with the regulator **G**.

## 5. Experimental testing of the designed controller

Both the gain scheduling scheme with PD and the robust controller **G** were able to generate good MSI reduction percentages in simulation. Testing of the control designs done for decreasing MSI in the process (vertical dynamics of a high-speed ship plus the dynamics of its actuators), mainly consisted of sea behaviour trials in CEHIPAR (El Pardo Model Basin, Spain) at 40 knots and sea state number SSN = 4, 5 with a scaled down replica $\frac{1}{25}$ the size of a high-speed ferry, to which a pair of Flaps had been added onto the stern, and a T-foil onto the bow (see Fig. 1).

Table 4 presents the MSI reduction percentages obtained with gain scheduling schemes using PD controllers, and with the robust controller **G**. It can be seen that in nominal conditions with the two multivariable controllers, very similar MSI reduction percentages of around 56% were obtained. In the case of SSN = 5, the greatest MSI reduction percentage that were obtained with PD controllers was around 42%, while with the QFT MIMO control the minimum reduction obtained was 22.5%.

It is also interesting to compare the MSI reduction percentages obtained in simulation (see Table 3) with the MSI reduction percentages obtained in sea behaviour trials (see Table 4). At 40 knots with PD controllers, the MSI reduction percentages are lower in sea behaviour trials than in simulation. With the QFT MIMO control, the opposite

Table 4
Reduction percentages of the MSI obtained in the sea behaviour trials using a gain scheduling scheme with PD and the designed controller **G**

| ($U$,SSN) | MSI(PD) (%) | MSI(**G**) (%) |
|---|---|---|
| (40,4) | 55.6 | 56.0 |
| (40,5) | 42.3 | 22.5 |

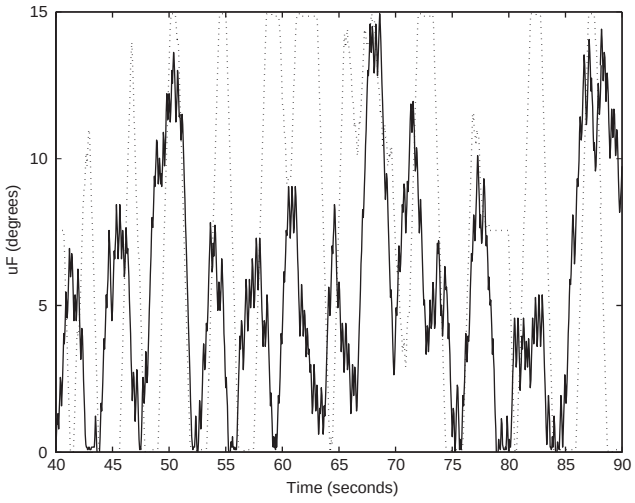


Fig. 13. Position of the flaps measured in a sea behaviour trial at $U = 40$ knots and SSN = 4 using a PD on heave- PD on pitch (broken line) and using the controller **G** (solid line).

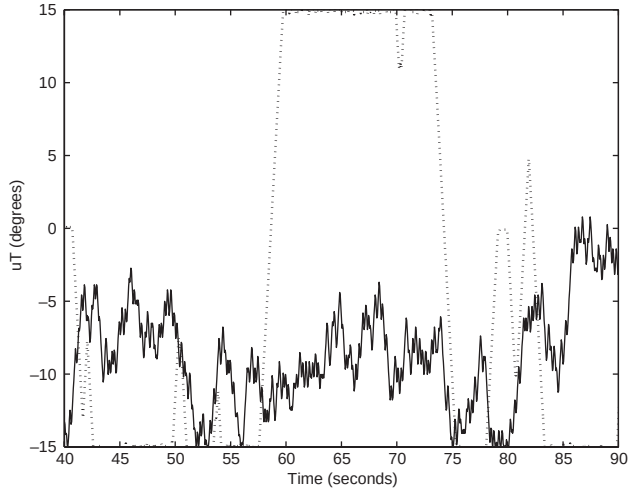


Fig. 14. Position of the T-foil measured in a sea behaviour trial at $U = 40$ knots and SSN = 4 using a PD on heave- PD on pitch (broken line) and using the controller **G** (solid line).

is true. This contradiction is due to the process model used in simulation that is only an approximation of the real process. The tuning of the PD controllers is very dependent on the process model. This dependency does not occur with QFT MIMO control, due to its robust nature.

Fig. 13 and Fig. 14 show the position of the flaps and the T-foil, respectively measured in a sea behaviour trial at 40 knots and SSN = 4 using the classic multivariable controllers (PD) and the robust controller **G**. The saturation of both actuators is very high using the PDs, while with the robust controller **G** there is no saturation. This behaviour is basically to be expected since the controller **G** was designed to assure a moderate saturation.

Finally, Fig. 15 shows the vertical acceleration obtained in sea behaviour trials at nominal conditions, with no control and using the robust controller **G**. A 32% reduction is achieved using this regulator. The random nature of the

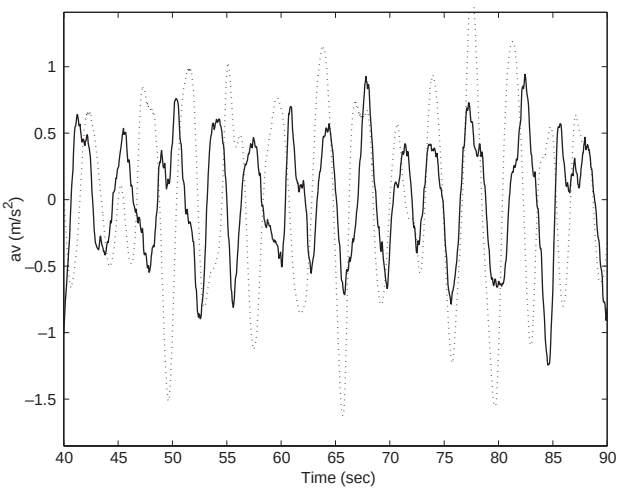


Fig. 15. Vertical acceleration obtained in a sea behaviour trial at $U = 40$ knots and SSN = 4 of the process without control (broken line) and with the controller **G** (solid line).

waves prevents a reproduction of the same wave height time series in different sea behaviour trials. For this reason the decrease of the vertical acceleration obtained with the controller **G** is more difficult to appreciate in Fig. 15 than in Fig. 11.

## 6. Conclusions

This work serves as a pioneering contribution in the use of QFT methodology to the design of a controller for a high speed ship. We have improved the design of a multivariable robust controller **G** so that it will be able to reduce incidences of motion sickness on high speed ferries. Motion sickness is caused by vertical accelerations associated with the heave and pitch motions induced by waves.

Testing of the controller in sea behaviour trials using a scaled down replica $\frac{1}{25}$ the size of a high-speed ferry in CEHIPAR has shown the validity of the design, since acceptable MSI reduction percentages have been obtained similar to those foreseen in simulation.

The designed controller **G** has been compared with a previous one—a gain scheduling scheme with PD. The comparison has shown that the system controlled with **G** has got robust performance and presents low saturation of the actuators, while the system controlled with a gain scheduling scheme with PD presents a higher saturation and has not got robust performance.

Nevertheless, reductions in MSI were observed as greater at two specific working points with the gain scheduling scheme. Under nominal conditions, they were virtually the same as those obtained with the robust design. This result was to be expected since QFT methodology works with a large family of plants giving rise to a robust control design, which ensures some minimum features for all the family plants. It is a more conservative design than the gain scheduling scheme, which uses classic controllers tuned exclusively at four working points.

In theory, the design of a gain scheduling scheme with PD controllers seems simpler than the robust design with QFT. However, the heavy dependence on using a process model to syntonise the PD makes it necessary to resyntonise several times. This in effect make its use more complex than the QFT design.

## Acknowledgements

This development was supported by CICYT of Spain under contract DPI2003-09745-C04-01.

## References

Aranda, J., Díaz, J.M., Ruipérez, P., Rueda, T.M., & López, E., (2001). Decrease in of the motion sickness incidence by a multivariable classic control for a high speed ferry. *Proceedings of IFAC Conference on Control Applications in Marine Systems 2001 (CAMS 2001)*. Glasgow, (UK): Pergamon Press.

Aranda, J., Cruz, J. M., & Díaz, J. M. (2004). Identification of multivariable models of fast ferries. *European Journal of Control*, *10*(2), 187–198.

Borghesani, C., Chait, Y., & Yaniv, O. (1995). *Quantitative feedback theory toolbox—for use with MATLAB*. Natick, MA: The MathWorks Inc.

Cruz, J. M., Aranda, J., Giron-Sierra, J. M., Velasco, F., Esteban, S., Díaz, J. M., & Andres-Toro, B. (2004). Improving the comfort of a fast ferry, smoothing a ship's vertical motion with the control of flaps and T-foil. *Control Systems Magazine*, *24*(2), 47–60.

Díaz, J.M., (2002). *Identification, Modelling and control of the vertical dynamics of a high speed ship*. Doctoral Thesis (in Spanish), Departmentof Computation and Automatica, UNED, Madrid( Spain).

Dormido, S., Aranda, J., Díaz, J.M., & Dormido Canto, S., (2001). Interactive educational environment for design by QFT methodology. In: M. García-Sanz (Ed.), *Proceedings of Fifth International Symposium on Quantitative Feedback Theory and Robust Frequency Domain Methods*. Pamplona (Spain).

Esteban, S., Girón-Sierra, J. M., Cruz, J. M., Andrés, B., Díaz, J. M., & Aranda, J. (2000). Fast ferry vertical accelerations reduction with active flaps and T-foil. In Blanke, M., Pourzajani, M. M. A., & Vukic, Z. Z. (Eds.), *Proceedings of Fifth IFAC Conference on Manoeuvring and Control of Marine Craft (MCMC2000)*. Aalborg (Norway): Pergamon Press.

Horowitz, I. M. (1963). *Synthesis of feedback systems*. New York: Academic Press.

Horowitz, I. M. (1992). *Quantitative feedback design theory (QFT)*. 660 South Monaco Dorkway Denver, Colorado: QFT Publishers.

Horowitz, I. M. (2001). Survey of quantitative feedback theory (QFT). *International Journal of Robust and Nonlinear Control*, *11*(10), 887–921.

Houpis, C. H., Sating, R. R., Rasmussen, S., & Sheldon, S. (1994). Quantitative feedback theory technique and applications. *International Journal of Control*, *59*, 39–70.

Houpis, C. H., & Rasmussen, S. J. (1999). *Quantitative feedback theory: fundamentals and applications*. New York: Marcel Dekker.

O'Hanlon, J. F., & McCauley, M. E. (1974). Motion sickness incidence as a function of the frequency and acceleration of vertical sinusoidal motion. *Aerospace Medicine*, *45*(4), 366–369.

Piguet, Y. (1999). *Sysquake user manual, version 1.0*. Lausanne, Switzerland: Calerga.

Vidyasagar, M. (2001). Randomized algorithms for robust controller synthesis using statistical learning theory. *European Journal of Control*, *7*(2–3), 287–310.

Yaniv, O. (1999). *Quantitative feedback design of linear and nonlinear control systems*. Norwell, Massachusetts: Kluwer Academic Publishers.